CONSTRAINT SINGULARITIES AS CONFIGURATION SPACE SINGULARITIES

DIMITER ZLATANOV, ILIAN A. BONEV AND CLÉMENT M. GOSSELIN
Laboratoire de robotique, Université Laval, Québec, QC, Canada G1K 7P4
[zlatanov, bonev, gosselin]@gmc.ulaval.ca

Abstract This paper examines the phenomenon of constraint singularity of a parallel mechanism, as defined in a recent publication. We focus our attention on the fact that constraint singularities are always singular points of the configuration space of the kinematic chain. As such, they separate distinct configuration space regions and may allow transitions between dramatically different operation modes. All this is exemplified by a multi-operational parallel mechanism that can undergo a variety of transformations when passing through singular configurations.

1. Introduction

A *constraint singularity* is a configuration of a parallel mechanism with $n < 6$ dof, where both the mechanism as a whole and the moving platform have at least $n + 1$ dof (Zlatanov et al., 2002). By definition, a constraint singularity is always an IIM-type singularity (Zlatanov et al., 1994) , i.e., a configuration with *increased instantaneous mobility* (IIM).

IIM-type (or *uncertainty*, Hunt, 1978) configurations are the singular points of the configuration space ($\mathcal{C}$-space) of a mechanism. The $\mathcal{C}$-space is the set of all possible configurations, i.e., the feasible arrays of joint-parameter values. For a closed-loop kinematic chain, the $\mathcal{C}$-space is a subset of the joint-space manifold, but not necessarily a submanifold; it may have points with no Euclidean neighbourhoods. These $\mathcal{C}$-singularities are associated with what can be described as "branching" or "self-intersection" of the $\mathcal{C}$-space. A motion starting at such a point can end up in any one of the meeting $\mathcal{C}$-space "sheets". The behaviours of the mechanism in bordering nonsingular regions can be quite different. At a constraint singularity the adjoining regions of the $\mathcal{C}$-space can be expected to sometimes allow different systems of platform freedoms and, therefore, result in distinct modes of operation of the mechanism.

This paper studies how constraint and IIM singularities connect neighbouring $\mathcal{C}$-space regions. The example used is a parallel chain that undergoes fascinating transformations when moving through a constraint singularity from one 3-dof part of its $\mathcal{C}$-space to the next.

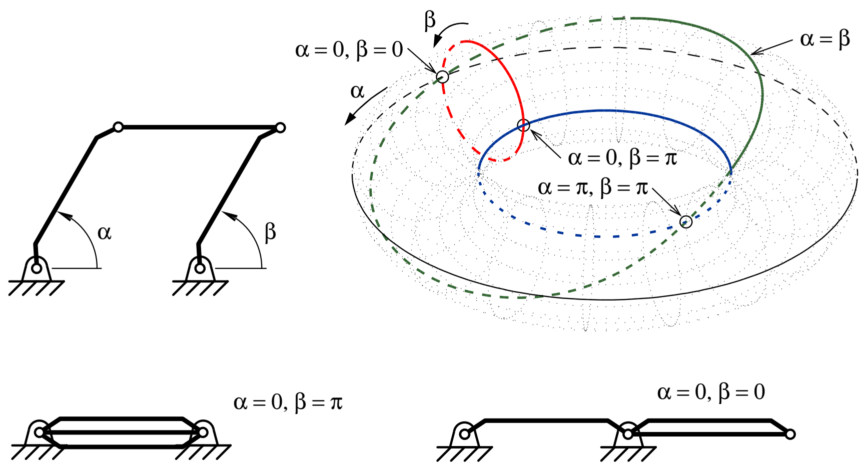

Figure 1. The equal-length four-bar mechanism, the $\mathcal{C}$-space and its singularities.

2. $\mathcal{C}$-space Singularities as Branching Points

Possibly the simplest interesting example of a $\mathcal{C}$-space singularity is a flattened four-bar linkage. As it was pointed out in (Zlatanov et al., 2002), this IIM configuration is a constraint singularity if the output link (the end-effector) is the *coupler* (since it has two transitory dof).

When all four bars have different lengths, the $\mathcal{C}$-space is homeomorphic to the figure eight, i.e., topologically it may be described as two circles joined by a single common point (the flattened configuration). The $\mathcal{C}$-space has two disjoint open connected nonsingular parts, and the mechanism can switch from one to the other (only) by passing through the IIM singularity. The two regions correspond to two different 1-dof sets of poses of the coupler. However, in both regions the allowed instantaneous coupler motion will be of the same type—an instantaneous rotation. (The screw system of the output freedoms remains the same.)

When all four bars are equal (Fig. 1), there are three constraint singularities, where the coupler has two instantaneous dof. The $\mathcal{C}$-space of a four-bar can be easily illustrated since it has a faithful projection on a torus, a configuration being defined in a unique way by (α, β), the base joint angles. Three smooth curves on the torus ($\alpha = 0$, $\beta = \pi$, and $\alpha = \beta$) form the $\mathcal{C}$-space; their intersection points are the singularities. These three points divide the $\mathcal{C}$-space into six non-singular regions.

In Fig. 1, two distinct regions of the $\mathcal{C}$-space may allow completely different coupler motions. While on one of the curves, $\alpha = \beta$, (i.e., in two of the $\mathcal{C}$-space regions) the coupler remains parallel to the base, on each of the other two curves (four regions) the coupler rotates about a point fixed in the base. At two singularities the mechanism has the options of entering two translational and two rotational regions, while at the third point the four-bar can choose among four rotational regions. We could say that the mechanism can be used both as a translational and as a rotational device and the transition between the two modes of operation may occur when the device goes through a constraint singularity.

Such "multi-functionality" is not limited to four-bars.

3. The DYMO Parallel Mechanism

The mechanism in Figs. 2–4 is a parallel chain with three *URU* legs. The centres (A, B, C) of the three platform U-joints form an equilateral triangle and so do the base U-joint centres. For each leg, we denote the revolute-joint screws by $\boldsymbol{\varrho}_i^P$, $i = 1, \ldots, 5$, $P = A, B, C$. The three base joint axes, $\boldsymbol{\varrho}_1^P$ meet (to form a "Y") at the base centre, O, and so do the last R-axes, $\boldsymbol{\varrho}_5^P$, at the platform centre, Q. The three intermediate R joints in each leg are parallel. The base frame is at O with a (vertical) z axis normal to the base plane π_b. We will refer to the manipulator as the *3-URU Double–Y Multi-Operational (DYMO)* parallel mechanism.

Since there are 15 joints, all revolute, the $\mathcal{C}$-space is a three-dimensional subset of a 15-torus. To avoid unnecessary complexity, we will not distinguish between configurations with the same pose of the platform and directions of the axes of $\boldsymbol{\varrho}_3^P$ (recall that $\boldsymbol{\varrho}_2^P \parallel \boldsymbol{\varrho}_3^P \parallel \boldsymbol{\varrho}_4^P$). Given a generic platform pose, there are 4 different solutions for the posture of each leg, and hence 64 different configurations of the mechanism as a whole. The distinction between these will not be essential for our purposes. Therefore, we assume that the ambient manifold, where our $\mathcal{C}$-space is embedded, is the Cartesian product of $SE(3)$ and 3 copies of the projective line, $\mathbb{R}P^1$. (We do not distinguish between $\boldsymbol{\varrho}_5^P$-joint angles that differ by 180°, hence the $\mathcal{C}$-space of the joint is $\mathbb{R}P^1$ rather than a circle.)

We will now proceed to examine the $\mathcal{C}$-space of the kinematic chain in a way similar to the analysis of the folding four-bar in Section 2. The goal is to identify the $\mathcal{C}$-space singularities and the non-singular $\mathcal{C}$-space regions. We want to know which $\mathcal{C}$-singularities are constraint singularities, what end-effector motions are possible in each non-singular region and what forms of transition exist between these regions.

4. Two Translational Mechanisms

It is no surprise that the mechanism can be translational in part of its $\mathcal{C}$-space (Fig. 2a). Translational manipulators of this type are well known (Appleberry, 1992, Tsai, 1996). Their singularities were studied by Di Gregorio and Parenti-Castelli, 1998.

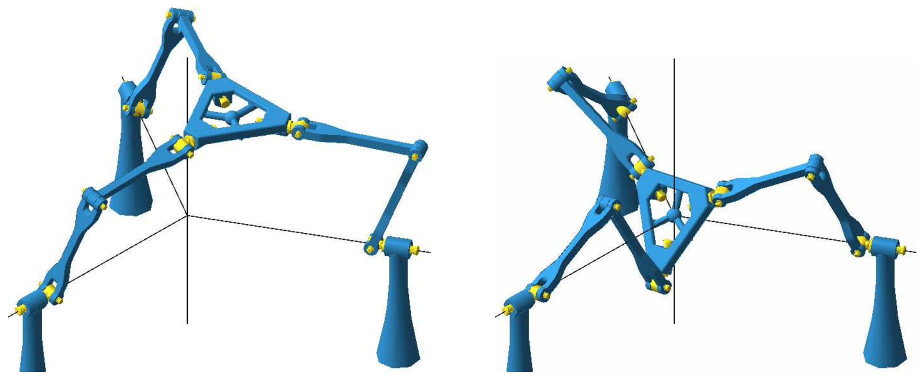

(a) (b)

Figure 2. The DYMO chain in (a) translation mode and (b) orientation mode.

When a leg, P, is nonsingular ($\boldsymbol{\varrho}_i^P$ are linearly independent) it imposes one constraint, $\boldsymbol{\zeta}^P$, on the platform. The wrench $\boldsymbol{\zeta}^P$ is either a force, $\boldsymbol{\varphi}^P$, parallel to $\boldsymbol{\varrho}_3^P$ and passing through the intersection of $\boldsymbol{\varrho}_1^P$ and $\boldsymbol{\varrho}_5^P$, or, if $\boldsymbol{\varrho}_1^P \parallel \boldsymbol{\varrho}_5^P$, a pure moment, $\boldsymbol{\mu}^P$, perpendicular to all $\boldsymbol{\varrho}_i^P$. The total constraint system is $\mathcal{W} = \mathrm{Span}\,(\boldsymbol{\zeta}^P | P = A, B, C)$ and the platform freedom system is $\mathcal{T} = \mathcal{W}^\perp$. If a leg is singular, it imposes additional constraints. A constraint singularity occurs when $\dim \mathcal{W} < 3$. A $\mathcal{C}$-singularity also occurs when there are singular legs leading to d instantaneous dof in the legs *with a fixed platform* and $\dim \mathcal{W} < 3 + d$. We will not consider configurations where a leg is fully extended or folded, but will examine cases with $\boldsymbol{\varrho}_1^P = \boldsymbol{\varrho}_5^P$ (for exactly one or all three P) where a singular leg can freely spin when the platform is fixed.

Let the platform have zero orientation (parallel Ys), and no leg be singular, Fig. 2a. Then, $\boldsymbol{\zeta}^P = \boldsymbol{\mu}^P$, $\forall P$. It can be shown that the three moments $\boldsymbol{\mu}^P$ will remain linearly independent unless one of two things happens: (a) $Q \in Oz$; or (b) the platform plane, π_p,coincides with the base, $\pi_p \equiv \pi_b$, i.e., $Q \in \pi_b$. The intersection of (a) and (b) must be treated as a separate case (c) $Q \equiv O$. We can conclude that once the platform is assembled with zero orientation this will not change until a configuration defined by conditions (a) or (b) is reached.

Case (a) corresponds to a constraint singularity described in (Zlatanov et al., 2002). It is an IIM configuration where both the platform and the mechanism as a whole have five instantaneous dof; $\mathcal{T}$ includes all translations and the rotations with horizontal axes.

In case (b) ($\pi_p \equiv \pi_b$), $\boldsymbol{\mu}^P, P = A, B, C$, become coplanar and the platform acquires the capability to rotate about any vertical axis. The mechanism as well as the platform will generally have 4 dof. If $Q \in \boldsymbol{\varrho}_3^P$ for one P, then the mechanism will still have 4 dof but the platform will have only 3 dof. Indeed, when Q is on the base Y, but not at O, ∞^1 configurations for a fixed platform are obtained while the leg spins. However, only one of those configurations, where $\boldsymbol{\varrho}_3^P \parallel Oz$, $\forall P$, is a $\mathcal{C}$-space singularity. In this case the mechanism has 4 dof but the platform only three, two horizontal translations and a vertical rotation.

Case (c), when the two Ys coincide, corresponds to infinitely many translation-mode configurations. Indeed, all legs can spin while base and platform coincide forming a 3-torus of $\mathcal{C}$-space points. Not all are adjacent to translation-mode regions—these points form a 2-surface on T^3. This situation is further addressed in Section 7.

Note that there are $\mathcal{C}$-space singularities, of cases (b) and (c), for all positions of Q in π_b. Yet, this does not disconnect the set of nonsingular zero-orientation translation-mode configurations. There exist paths that avoid $\mathcal{C}$-space singularities and join configurations on both sides of the base plane. For such paths, Q passes through π_b in a point along the base Y (but not O). As we pointed out above, such configurations are not $\mathcal{C}$-space singularities as long as the single singular leg is not in the base plane. Moreover, note that each such configuration has a neighbourhood of non-singular $\mathcal{C}$-space points. Hence, the non-singular $\mathcal{C}$-points with zero platform orientation form a connected open set.

It is now time to observe that everything written since the beginning of the present section is valid if "zero orientation" becomes "180°-yaw orientation". Hence, there are two translation-mode regions (with different orientations). They have no common boundary points but, as we will see, there are continuous $\mathcal{C}$-space paths between them.

5. An Orientational Mechanism

In (Zlatanov et al., 2002) we discussed a 3-*UPU* parallel wrist proposed by Karouia and Hervé (2000) and analyzed by Di Gregorio (2001). The link-geometry condition is that the base R joints intersect in a common point and so do the platform R joints. DYMO satisfies this condition, therefore it has an orientation mode of operation (Fig. 2b).

Assume that $Q \equiv O$ and no leg is singular, Fig. 2b. For each P, the constraint $\boldsymbol{\zeta}^P = \boldsymbol{\varphi}^P$ is a force through O parallel to $\boldsymbol{\varrho}_3^P$. When $\boldsymbol{\varphi}^P$, $P = A, B, C$, are linearly independent, the freedom system, $\mathcal{T}$, is the 3-system of all rotations about O. When the forces $\boldsymbol{\varphi}^P$ become coplanar the platform also acquires the freedom to translate in a direction orthogonal to the plane of the constraints. Such a configuration will then be a constraint singularity since the platform will have at least 4 dof (if all three forces are parallel, which can happen only if $\pi_p \equiv \pi_b$, the platform acquires *two* horizontal translations for a total of 5 dof).

Careful analysis reveals that the $\mathcal{C}$-space singularities adjacent to the orientation mode are the configurations with *zero-yaw* platform orientation, i.e., they are obtained from orientation zero by a single (finite) rotation with a horizontal axis (a tilt in the vertical plane of some azimuth). All such orientations correspond to $\mathcal{C}$-space singularities.

However, if the axis of the finite (non-zero) tilt is along $\boldsymbol{\varrho}_1^P$, then there are infinitely many configurations (due to leg spinning) and not all of them lead to coplanar constraints and singularity. Only one of the orientations of the spinning leg (for every half-turn) is a constraint singularity, while for any other the configuration is non-singular.

The exact singularity identification for this mode was performed using the *modified Euler angles* as introduced in (Bonev and Ryu, 1999).This formulation yields simpler symbolic expressions and also helped to establish that the IIM singularities divide the set of non-singular *orientations* of the platform into two disjoint connected components (with positive and negative yaw angle, respectively). However, the $\mathcal{C}$-singularity surface does not disconnect the set of non-singular *configurations* in the orientation mode. This is in close analogy to the translation mode and its singularities with $Q \in \pi_b$. There are non-singular orientation-mode paths that cross the singularity surface from positive to negative yaw via any configuration where the tilt axis is one of the base R-joints. Thus, the non-singular orientation-mode $\mathcal{C}$-space points form a connected set.

We can now resolve one transition question from the previous section. Assuming that the leg length is sufficient, it is possible to move continuously between two translation-mode configurations with opposite yaw angles via the orientation mode.We will see later that this is not the only route between the two translation modes.

6. Two Mechanisms for Planar Motion

In translation mode, we saw that if the platform is put in π_b it acquires as a fourth dof a vertical-axis rotation. In orientation mode, when $\boldsymbol{\varphi}^P$, $P = A, B, C$, are vertical, the platform gains the horizontal translations.

In both cases, $\mathcal{T}$ includes as a subsystem the planar motions, $\mathcal{E}$. It is obvious that the capacity for planar motion is not transitory and that finite planar motions can originate from the described configurations. Indeed one glance at the mechanism should suffice to immediately recognize the features of a 3-RRR planar parallel manipulator (Fig. 3a).

If $\pi_p \equiv \pi_b$ and no leg is singular, $\boldsymbol{\varrho}_i^P$, $i = 2, 3, 4$, $P = A, B, C$ are vertical. Therefore, each $\boldsymbol{\zeta}^P$ is either a vertical force or a horizontal moment, and $\mathcal{T} \supset \mathcal{E} = \mathcal{E}^\perp \supset \mathcal{W}$. It must be observed that the above is true not only when the platform is in π_b "*face up*" but also "*face*

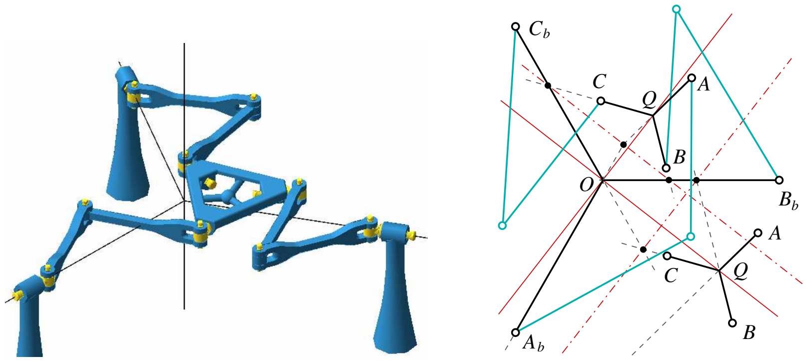

(a) (b)

Figure 3. The planar mode: (a) face up; (b) $\mathcal{C}$-singularities face down.

down", although then the 3-RRR planar parallel mechanism will be less recognizable since the base and platform attachment points will be in reverse circular order. So there are two planar modes, which obviously do not have common adjacent configurations, yet it is still possible to go with a continuous motion from one to the other via the orientation mode. We will see later that there is another route as well.

If $O \not\equiv Q$, $\mathcal{W}$ degenerates when either: (a) $\boldsymbol{\zeta}^P = \boldsymbol{\varphi}^P$, $\forall P$, and the two Ys intersect in three collinear points; (b) $\boldsymbol{\zeta}^P = \boldsymbol{\mu}^P$, $\forall P$ (the Ys are parallel); (c) say $\boldsymbol{\zeta}^A = \boldsymbol{\mu}^A$ and the other two are forces whose plane is perpendicular to $\boldsymbol{\mu}^A$. Cases (a) and (c) require the two Ys to be mirror images and occur only when π_p is face-down, (b) is possible only face-up.

Therefore, the face-up $\mathcal{C}$-singularities occur when: (i) the platform orientation is $\psi = 0$ or $\psi = \pm\pi$, (constraint singularities adjoining the translation mode if no pair $(\boldsymbol{\varrho}_1^P, \boldsymbol{\varrho}_5^P)$ is aligned); (ii) $O \equiv Q$, ($\mathcal{C}$-singularities adjoining the orientational mode). The $\mathcal{C}$-singularities divide the face-up planar mode into two regions ($\psi < 0$ and $\psi > 0$).

It can be shown that the face-down singularities correspond to the following platform poses. For every orientation, the singular locations of Q are given by a pair of perpendicular lines through the origin. Fig. 3b shows such a cross at O and two singular poses ($A_b B_b C_b$ is the base). The orientation of this cross changes with the orientation of the platform, only twice slower. The singularity surface formed by the rotating cross divides the face-down planar mode into four component regions. In both (a) and (c) the platform acquires a rotation about a horizontal axis. This is both the line of the application points of the constraint forces and the axis of symmetry of the two Ys (the dash-dot lines for each pose, Fig. 4b). These singularities border neither translational nor orientation regions. They allow the mechanism to escape into a mixed mode of operation.

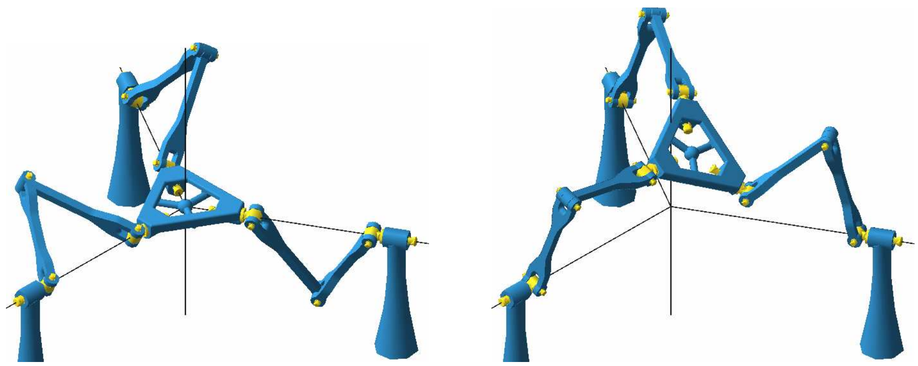

(a) (b)

Figure 4. The DYMO chain in (a) lockup mode and (b) mixed mode.

7. Two Lockup Poses

Let $Q \equiv O$ and the platform be horizontal, face-up, and with $\psi = 0$ or $\psi = \pi$ (Fig. 4a). Since all legs can spin independently, there are two 3-tori of such configurations. For most of them, the mechanism has 3 dof but the platform cannot move. Each T^3 has ∞^3 dead-point configurations where the platform is "stuck." We can say that the tori are two separate "modes of operation," with $\mathcal{T} = 0$.

In this mode, there are $\mathcal{C}$-space singularities where the platform acquires a freedom and can escape the lockup pose. Each leg imposes two constraints, a force, $\boldsymbol{\varphi}^P$, and a moment, $\boldsymbol{\mu}^P$. There are two types of IIM singularities: (a) the three $\boldsymbol{\mu}^P$ are co-planar and the platform can escape into orientation mode; (b) the $\boldsymbol{\varphi}^P$ are coplanar and the platform can translate in the z direction and switch to translation mode. There are two singularities where the platform acquires 3 dof, the mechanism as a whole has 6 dof and both (a) and (b) are satisfied. When all $\boldsymbol{\varrho}_3^P$ are vertical, the platform has 3 dof and it can escape with any planar motion. When $\boldsymbol{\varrho}_3^P$ are horizontal, the platform also has 3 dof: the rotations with axes in π_b and the vertical translation.

8. A New Mechanism with Mixed Freedoms

At several occasions we described singularities where DYMO has instantaneous motions which do not lead into the so-far listed operation modes. In Section 4, case (a) ($Q \in Oz, Q \not\equiv O$, zero orientation), the singularity allows two rotational freedoms but it is not adjacent to the orientational mode. Similarly, an orientation-mode constraint singularity allows translations with non-zero tilt of the platform (Section 5). In fact, these freedoms can be part of finite motions into $\mathcal{C}$-space regions with $Q \not\equiv O$ and $\pi_p \nparallel \pi_b$, where the mechanism works as a new manipulator with three mixed freedoms, Fig. 4b. (Yet, a similar chain appears in (Hunt, 1973) as a constant velocity shaft coupling.)

It has been possible to describe completely the configurations in the mixed mode. The process is very interesting but the description cannot be made within the limits of this paper. Below we present an overview of the results and invite the reader to visit the Para*ll*eMIC website, where a more detailed analysis as well as video demonstrations can be found (`http://www.parallemic.org/Reviews/Review008.html`).

A key in the analysis of the mixed mode is the observation that for any feasible configuration with $Q \not\equiv O$ and $\pi_p \nparallel \pi_b$ the translation along OQ is a platform freedom. This is a finite freedom and it provides a route of entry from mixed into orientation mode. The freedom and constraint systems in a mixed-mode configuration are given by the same 4th special screw 3-system. It is composed of all zero-pitch screws in the plane bisecting π_p and π_b, as well as the infinite pitch screws perpendicular to it and parallel to OQ.

The mixed-mode configuration set is axisymmetric with respect to Oz. For every azimuth, there are configurations with arbitrary tilt between $0°$ and $180°$. For all configurations with given azimuth and tilt (ϕ, θ), Q is along a ray from O with azimuth and tilt $(\phi, \theta/2)$.

Thus, along the vertical axis we have tilt zero; along rays inclined at $45°$ are the configurations with tilt $90°$, i.e., with vertical platform facing away from the central axis; and along rays in π_b the tilt angle is $180°$, i.e. the platform is face down and entering the face-down planar mode. This construction can be performed both starting with zero orientation and with a platform yawed at $180°$ (about the platform normal). In other words for every feasible configuration of the mixed mode there is another with a platform rotated at $180°$ about its normal axis. Furthermore, there are poses on both sides of π_b.

The mixed-mode $\mathcal{C}$-space singularities occur for: (a) $Q \in Oz$, adjacent to the two translation modes; (b) $Q \equiv O$, on the orientation mode boundary; and (c) $Q \in \pi_b$, common with the face-down planar mode. Those in (c) disconnect the mixed-mode $\mathcal{C}$-space into four adjacent regions. The mixed mode provides connecting paths between the two translation modes, as well as the face-up and face-down planar modes.

9. Conclusions

The analyzed mechanism has a configuration space with multiple 3-dimensional regions separated by surfaces of $\mathcal{C}$-space singularities. These regions allow for five dramatically different types of platform motion, yet transition between the modes of operation is possible without disassembly. There is little doubt that this type of behaviour is exhibited by many other mechanisms with reduced freedoms.

10. Acknowledgements

The authors would like to thank Mr Pierre-Luc Richard and Mr Thierry Laliberté for their work on the CAD model and the plastic prototype of DYMO. The financial support of the Canada Research Chair Programme and NSERC is also acknowledged.

References

Appleberry, W.T., 1992, "Anti-rotation positioning mechanism," *U.S. Patent No. 5,156,062*.

Bonev, I.A., and Ryu, J., 1999, "Orientation Workspace Analysis of 6-DOF Parallel Manipulators," *ASME Design Engineering Technical Conferences*, DAC-8646, Las Vegas, September 12-15.

Di Gregorio, R., and Parenti-Castelli, V., 1998, "A Translational 3-DOF Parallel Manipulator," *Advances in Robot Kinematics: Analysis and Control*, J. Lenarcic and M.L. Husty (eds.), Kluwer Academic Publishers, pp. 49-58.

Di Gregorio, R., 2001, "Statics and Singularity of the 3-UPU Wrist," *Proceedings of the IEEE/ASME International Conference on Advanced Intelligent Mechatronics*, Como, Italy, pp. 470-475, July 8-12.

Hunt, K. H., 1973, "Constant-velocity shaft couplings: a general theory," *Transactions of the ASME, Journal of Engineering for Industry*, Vol. 95B, pp. 455-464.

Hunt, K.H., 1978, *Kinematic Geometry of Mechanisms*, Oxford University Press.

Karouia, M., and Hervé, J.M., 2000,"A Three-DOF Tripod For Generating Spherical Rotation," *Advances in Robot Kinematics*, J. Lenarcic and M.M. Stanisic (eds.), Kluwer Academic Publishers, pp. 395-4020.

Tsai, L-W., 1996, "Kinematics of a Three-DOF Platform With Three Extensible Limbs," *Recent Advances in Robot Kinematics*, J. Lenarcic and V. Parenti-Castelli (eds.), Kluwer Academic Publishers, pp. 401–410.

Zlatanov, D., Benhabib, B. and Fenton, R.G., 1994, "Singularity Analysis of Mechanism and Robots Via a Velocity-Equation Model of the Instantaneous Kinematics," *Proceedings of the IEEE International Conference on Robotics and Automation*, San Diego, CA, pp. 986-991.

Zlatanov, D., Bonev, I.A., Gosselin, C.M., 2002, "Constraint Singularities of Parallel Mechanisms," accepted for publication, *Proceedings of the IEEE International Conference on Robotics and Automation*, Washington, DC, May 12-15. Available online: `http://wwwrobot.gmc.ulaval.ca/~zlatanov/CS.ps`